arXiv:1704.04273v1 [cond-mat.str-el] 13 Apr 2017

Finite-size anomalies of the Drude weight: role of symmetries and ensembles

R. J. Sánchez[1] and V. K. Varma[2,3,4,5]

[1]*Bethe Center for Theoretical Physics, Universität Bonn, Germany*
[2]*The Abdus Salam ICTP, Strada Costiera 11, 34151, Trieste, Italy*
[3]*Initiative for the Theoretical Sciences, The Graduate Center, CUNY, New York, NY 10016, USA*
[4]*Department of Engineering Science and Physics, College of Staten Island, CUNY, Staten Island, NY 10314, USA*
[5]*Department of Physics and Astronomy, University of Pittsburgh, Pittsburgh, PA 15260, USA*

(Dated: April 17, 2017)

We revisit the numerical problem of computing the high temperature spin stiffness, or Drude weight, D of the spin-1/2 XXZ chain using exact diagonalization to systematically analyze its dependence on system symmetries and ensemble, for various anisotropies Δ. At the isotropic point and in the gapped phase ($\Delta \geq 1$), D is found to vanish in the thermodynamic limit independent of symmetry or ensemble. In the gapless phase ($\Delta < 1$) and within the canonical ensemble for states with zero total magnetization, D vanishes exactly due to spin-inversion symmetry for all but the anisotropies $\tilde{\Delta}_{MN} = \cos(\pi M/N)$, with $N > 0$, $M < N$, provided system sizes $L \geq 2N$, for which states with different spin-inversion signature become degenerate, related to sl_2 quantum loop symmetry. Including a magnetic flux not only breaks spin-inversion but also lifts the degeneracies at the $\tilde{\Delta}_{MN}$ points. A finite-size scaling of D for different anisotropies, within both canonical and grand-canonical ensemble, and in the presence and absence of a magnetic flux is presented. The analysis demonstrates how convergence to the thermodynamic limit may be accelerated and the finite-size anomalies overcome: In the gapless phase our finite size results for D extrapolate nicely in the thermodynamic limit to recently computed exact lower-bounds provided spin-inversion symmetry is broken *or* the system size $L \geq 2N$.

I. INTRODUCTION

Ideal conduction is observed when the mean free path of particles exceeds the sample size and no scattering events occur. A key distinguishing feature between such ideal metals and other metals or insulators is their response to external dc fields: unimpeded acceleration of particles in the former produces a delta function in its conductivity with a certain spectral weight D, the Drude weight. A particularly convenient way to measure this quantity is through the response of the system's ground[1] or excited state[2–4] eigenfunctions to twisted boundary conditions: only ideal metals will produce a finite response, $D > 0$, to such a perturbation. While such *ballistic transport* is generically expected in integrable systems,[5] computing D even for simple models can often be done only numerically.[6–10]

In this work we compute D for a paradigmatic integrable quantum Heisenberg chain at high temperatures, for various combinations of the conserved symmetries and ensembles chosen. The important role of the model's discrete and dynamical symmetries in the numeric computation of D has been emphasized before.[6,8] We were motivated to revisit this long-studied problem due to certain inexplicable convergence rates of the finite system data to the thermodynamic limit found, for certain interaction strengths, in some of our own personal calculations as well as those in previous literature[7,9]; the details will be presented along the way. We attempt to resolve these issues by systematically enlisting the contributions of the current carrying states in each symmetry sector. In so doing we find what ensemble and what system symmetries (parity, spin-inversion, sl_2-loop symmetry) best help to achieve quickest convergence to the thermodynamic limit, and explicate why. We found this last point particularly relevant and revelatory in light of recent exact bounds and results[11,12] reported for the high-temperature Drude weight in this model.

At inverse temperature β, and in the absence of any singular long-time behavior of the current-current correlation function $\langle \hat{j}(t)\hat{j}(0)\rangle$, the Drude weight D has the spectral representation[4]

$$D(\beta) = \pi\beta \sum_n \frac{e^{-\beta E_n}}{LZ} \sum_{m, E_m = E_n} |\langle n|\hat{j}|m\rangle|^2, \qquad (1)$$

where E_i is the eigenvalue associated to the eigenstate $|i\rangle$ of the model and Z is the corresponding partition function. Let us remark here that we have explicitly confirmed the absence of any long-time plateau in the time-dependent part of the autocorrelation function $\langle \hat{j}(t)\hat{j}(0)\rangle$, which might arise from almost-degenerate states (ignored in the equation above), thereby validating the aforementioned assumption of nonsingular behaviour of the current autocorrelation function's oscillatory part.

In the following we shall numerically evaluate Eq. (1) for the spin-1/2 XXZ chain in the high-temperature limit, where the meaningful quantity is $\lim_{\beta\to 0} \beta^{-1} D(\beta)$.

II. MODEL AND SYMMETRIES

The spin-1/2 XXZ model with anisotropy $\Delta \geq 0$ and exchange integral J, for a L-site spin chain with periodic boundary conditions is described by the Hamiltonian

$$H = \sum_{j=1}^{L} \frac{J}{2} \left(\hat{S}_j^+ \hat{S}_{j+1}^- + \hat{S}_j^- \hat{S}_{j+1}^+ \right) + \Delta \, \hat{S}_j^z \hat{S}_{j+1}^z, \qquad (2)$$

where the ladder spin operators $(\hat{S}_j^+ \hat{S}_{j+1}^- + \hat{S}_j^- \hat{S}_{j+1}^+)$ flip pairs of spins at sites $j, j+1$.

The model is invariant under spin rotations $\hat{m}_z$ about the z-axis, lattice translations $\hat{T}$, and two discrete symmetries: (i) spin-inversion $\hat{Z}$ with eigenvalues $z = \pm 1$, defined such that

$$\hat{Z}|S_1^z, S_2^z, ..., S_L^z\rangle = |-S_1^z, -S_2^z, ..., -S_L^z\rangle, \qquad (3)$$

where $|S_1^z, S_2^z, ..., S_L^z\rangle$ labels the spin configurations of the chain; and (ii) space-reflection or parity $\hat{P}$, with eigenvalues $p = \pm 1$, defined as

$$\hat{P}|S_1^z, S_2^z, ..., S_L^z\rangle = |S_L^z, S_{L-1}^z, ..., S_1^z\rangle. \qquad (4)$$

Given that $\hat{m}_z$ commutes with $\hat{T}$, these two symmetry operations can be used to block-diagonalize Eq. (2). The resulting eigenstates can then be labeled by both the total magnetization m_z and the total crystal momentum K. On the other hand, the discrete symmetries can only be used for block diagonalization in specific subsectors[13]: (i) $\hat{Z}$ commutes with both $\hat{P}$ and $\hat{T}$ but only does so with $\hat{m}_z$ in the sector with zero total magnetization; (ii) $\hat{P}$ commutes with $\hat{m}_z$ but with $\hat{T}$ only in the subsectors with zero and π total crystal momentum.

Besides this set of symmetry operations, the periodic XXZ chain has additional symmetries at the dense set of commensurate "roots of unity" anisotropies $\tilde{\Delta}_{MN} = \cos(\pi M/N)$, with $N \in \mathbb{Z}^+$ and $M < N$, for which there exists a large class of zero-energy N-particle excitations.[14,15] These excitations give rise to degeneracies between a parent state with $m_z = m_z^{\max}$ and states with $m_z = m_z^{\max} - l\,N$, where $l \in \mathbb{Z}^+$. Deguchi et al.[14] numerically studied these degeneracies and found the corresponding multiplets have multiplicity

$$\begin{pmatrix} 2\, m_z^{\max}/N \\ l \end{pmatrix}, \qquad (5)$$

in the commensurable case $m_z = 0 \pmod N$, and

$$\begin{pmatrix} 2\,[m_z^{\max}/N] + \alpha \\ l \end{pmatrix}, \qquad (6)$$

in the incommensurable case $m_z \neq 0 \pmod N$, where $[x]$ is the greatest integer contained in x, and $\alpha = 0, 1$ or 2.

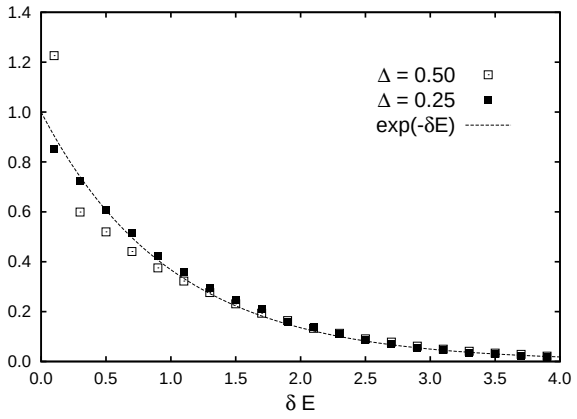

FIG. 1: XXZ 20-site chain level-spacing distribution for states within the sector of zero total magnetization, for two different anisotropies. The distribution is averaged over each spin-inversion sector z, for every crystal momentum, as well as over parities for $K = \{0, \pi\}$. Note the peak at $\delta E = 0$ for $\Delta = 0.5$ signaling the presence of additional degeneracies.

In particular, the degeneracies in the commensurable case were related to the sl_2-loop algebra,[14] whose generators commute with the XXZ Hamiltonian at roots of unity when $m_z = 0 \pmod N$. However, the incommensurable sectors do not have this symmetry. We shall refer to the quantum symmetry in the full Hilbert space by Λ.

The additional degeneracies in the system at these special $\tilde{\Delta}_{MN}$ points can be readily verified by inspecting the level spacing distribution.[16] Indeed, being an integrable model (i.e. exactly solvable by Bethe Ansatz) the XXZ chain has a macroscopic number of conserved quantities which allow to fully diagonalize the Hamiltonian. The resulting eigenvalues are statistically uncorrelated and their spacing distribution follows a Poisson distribution. In contrast, as shown in Fig. 1, at the commensurate anisotropy $\Delta = \tilde{\Delta}_{13} = 0.5$ the level spacing distribution deviates from the Poisson distribution and displays a small peak at $\delta E = 0$, signaling the presence of additional degeneracies.

We compute the spin stiffness (or Drude weight in the equivalent fermionic picture) of the XXZ model through Eq. (1). The "z" component of the current operator entering this equation is given by

$$\hat{j}^z = \sum_{j=1}^{L} i \frac{J}{2} \left(\hat{S}_j^+ \hat{S}_{j+1}^- - \hat{S}_j^- \hat{S}_{j+1}^+ \right), \qquad (7)$$

and it is odd under parity and spin-inversion, and even under translations and spin-rotations, i.e. $\hat{O}\hat{j}^z\hat{O} = \eta\, j^z$, where $\eta = -1$ for $\hat{O} = \hat{P}$, $\hat{Z}$ and $\eta = 1$ for $\hat{O} = \hat{T}$, $\hat{m}_z$.

Finally, to study the role of the discrete symmetries in the evaluation of Eq. (1), we break them using an irrational magnetic flux. The effect of threading the periodic spin chain with such a flux ϕ (we chose $\phi = \sqrt{2}$) is incorporated by gauging it into the spin-ladder operators

via the usual Peierl's substitution as $S^{\pm}_j \to e^{\pm i\phi j/L} S^{\pm}_j$. Hence it modifies both Eq. (2) and (7).

We shall find the present of the flux also lifts every $\tilde{\Delta}$-related degeneracy, as we will expatiate more fully in the next section.

III. RESULTS

The numerical evaluation of Eq. (1) may be performed either in the canonical or grand canonical ensemble. In the former case we sum over eigenstates with a fixed total magnetization m_z, whereas in the latter the summation includes eigenstates from all the different magnetization sectors. In what follows we consider only spin chains with even L.

Let us start by summarizing a couple of empirical observations regarding the many-body states connected by the current operator, Eq. (7), when the Drude weight is evaluated within the canonical ensemble. We shall see that when parity and spin-inversion symmetries are broken all nondegenerate eigenstates of Eq. (2) are eigenstates of the spin current operator, and that the main contribution to the Drude weight comes precisely from these nondegenerate states ($m = n$), with the degenerate states being only those coming from the Λ quantum symmetry at $\tilde{\Delta}_{MN}$. By contrast, if spin-inversion is present only Λ-related degenerate states contribute to D provided $L \geq 2N$. Table I recaps the main points we discuss below.

Current carrying states

Let us now describe the contribution from various current carrying states in the different magnetization sectors to D, and the influence of flux to these contributions.

(I) $m_z = 0$ **Sector**: due to the discrete symmetries present in this subsector, and to the oddness of the spin current under their action, only matrix elements from degenerate states of the form

$$\langle m, K, z|\hat{j}^z|-z, K, n\rangle, \quad \text{with} \quad K \neq \{0, \pi\}$$

or

$$\langle m, K, z, p|\hat{j}^z|-p, -z, K, n\rangle, \quad \text{with} \quad K = \{0, \pi\},$$

and $E_n = E_m$ contribute to the Drude weight, Eq. (1). For anisotropy values different from $\tilde{\Delta}_{MN}$ we find degenerate states only within the sectors of $K = \{0, \pi\}$. These states belong to different parity sectors but have the same spin-inversion signature and hence are not connected by the current operator. Therefore, there is no net current for any L and the Drude weight vanishes exactly in the sector of zero total magnetization. At the isotropic point ($\Delta = 1$) the $SU(2)$ symmetry was exploited to show explicitly that $D = 0$ for any β.[17]

For $\Delta = \tilde{\Delta}_{MN}$, on the other hand, we find degenerate states due to the additional quantum symmetry only for chains of size $L \geq L_{\min} \equiv 2N$, the number of which increases with system size. Indeed, the spectral degeneracies related to the Λ symmetry are split between sectors of $m_z = 0 \pmod N$.[14] For $N = 3$, for example, the first two magnetization sectors one needs to get any degeneracy are $m_z = (0, 3)$, and these are available only for chains with $L \geq 6$ ($= 2N$). More generally, the minimum length for the even-length chains we consider follows from Eq. (5). In fact, for the subsector of zero magnetization we can choose $m_z^{\max} = L/2$ and hence the smallest number of degenerate states is given by L/N (that is, choosing $l = 1$). Thus for $L = 2N$ one should find the first two degenerate states associated to the symmetries at $\tilde{\Delta}$, and we have checked numerically this is indeed the case (see table II for an example). Importantly, these states are pairwise degenerate with opposite spin-inversion (as well as opposite parity within the $K = \{0, \pi\}$ sectors) and yield a finite Drude weight.

This is the only case where degenerate contributions to D dominates over the nondegenerate contributions.

(II) $m_z \neq 0$ **Sector**: in the sectors of finite total magnetization there is no spin-inversion symmetry and hence every state potentially carries a current. The relevant matrix elements now are

$$\langle m, K|\hat{j}^z|K, n\rangle, \quad \text{with} \quad K \neq \{0, \pi\}$$

Symmetry	Current carrying states
$\hat{Z}$, $\hat{P}$ and Λ $\hat{Z}$ and Λ	Degenerate multiplets from Λ symmetry only.
$\hat{P}$ and Λ	All pairwise degenerate states of different parity, including Λ multiplets.
$\hat{Z}$ and $\hat{P}$ $\hat{Z}$	None.
$\hat{P}$	All pairwise degenerate states of different parity.
Λ	Every nondegenerate state, and the degenerate Λ multiplets.
None	Every nondegenerate state.

TABLE I: Current carrying states for blocks with fixed K and m_z, depending on the presence of spin-inversion $\hat{Z}$, parity $\hat{P}$, and quantum Λ symmetries.

L	$\deg(\Delta = 0.25)$	$\deg(\Delta = \tilde{\Delta}_{16})$
8	4	4
10	20	20
12	96	98
14	364	392
16	1364	1592

TABLE II: Number of degenerate states in the sector of zero total magnetization, for different system sizes and two anisotropy values. Note how the first two degenerate states due to the Λ symmetry appear at $L = 2N = 12$.

or

$$\langle m, K, p|\hat{j}^z| - p, K, n\rangle, \quad \text{with} \quad K = \{0, \pi\},$$

with $E_n = E_m$. For $\Delta \neq \tilde{\Delta}_{MN}$ and $K = \{0, \pi\}$, we find pairwise degenerate states of opposite parity, each of which are connected through the spin current operator. The rest of the K-subsectors have no degenerate states, but all of these are found to be eigenstates of the current operator and, consequently, to carry a finite current. Since all K-sectors are about the same dimension, it follows that the nondegenerate current-carrying states yield the dominant contribution to the Drude weight, an observation which has been made before.[8] For $\Delta = \tilde{\Delta}_{MN}$ one finds additional degeneracies in all K-subsectors. These additional degenerate states are not eigenstates of the current but do contribute to the Drude weight through off-diagonal terms.

(III) $m_z = 0$ **Sector and finite magnetic flux**: if $\Delta \neq \tilde{\Delta}_{MN}$ and $K = \{0, \pi\}$ we find the same number of degenerate states as for the non-fluxed model (flux breaks the symmetry between $\pm K$ states but $K = \{0, \pi\}$ sectors do not have corresponding counterparts). In this case, however, since parity and spin inversion are broken degenerate and nondegenerate states alike are eigenstates of the current operator and give finite contributions to the summation in Eq. (1). For all the other momenta one finds that all states are nondegenerate eigenstates of $\hat{j}^z$ and carry a finite current. Summarizing, the relevant matrix elements in this case are

$$\langle m, K|\hat{j}^z|K, n\rangle\, \delta_{mn}, \quad \text{with} \quad K \neq \{0, \pi\}$$

or

$$\langle m, K|\hat{j}^z|K, n\rangle, \quad \text{with} \quad K = \{0, \pi\},$$

with $E_n = E_m$. Remarkably, if $\Delta = \tilde{\Delta}_{MN}$ we find the presence of the flux lifts all the extra degeneracies coming from the additional quantum symmetry and hence the model behaves as though $\Delta \neq \tilde{\Delta}_{MN}$.

(IV) $m_z \neq 0$ **Sector and finite magnetic flux**: In this case we find no degenerate state in any of the symmetry subsectors, and that all the eigenstates of the model are also eigenstates of the current operator, and carry a finite current regardless of Δ. All contributing matrix elements, within any K-sector, therefore are of the form

$$\langle m, K|\hat{j}^z|K, n\rangle\, \delta_{mn}.$$

Drude weights

We present the infinite temperature Drude weight results in Fig. 2, evaluated within the grand canonical (GCE) and canonical ensemble (CE) in the $m_z = 0$ sector, both with and without a flux, for even-length chains of size $L = 6 - 18$. We also show a second order polynomial fit to the data points of $L = 10 - 18$ to guide the eye.

Per usual statistical mechanics GCE and CE should be equivalent in the thermodynamic limit, especially if the quantity measured is a meaningful one in this limit.[18] We will find that although in the gapped phase D quickly becomes independent of both ensemble and symmetries as L increases, in the gapless phase the presence of spin-inversion symmetry makes convergence towards the thermodynamic limit remarkably slow, depending on how fast the Λ degeneracies start showing up when increasing system size.

Gapless phase. — For $\Delta < 1$ it is rigorously known that the high temperature transport is ballistic[19] i.e. $D > 0$ in *any* magnetization sector, especially the zero magnetization sector where the Mazur's inequalities alone do not settle the issue. However computing the actual value of D in the gapless phase is a different matter, with D lower-bounded more strictly recently,[11] and even claimed to be exactly computable.[12] The explicit expression for the exact bound at the $\tilde{\Delta}_{MN}$ points reads

$$D \geq 2\pi \frac{\beta}{16} \frac{\sin^2(\pi M/N)}{\sin^2(\pi/N)} \left(1 - \frac{N}{2\pi} \sin(2\pi/N)\right). \qquad (8)$$

In the top panels of Fig. 2 we show the finite size data for $\beta^{-1}D$ as a function of system size in the gapless phase, for two anisotropies $\Delta = 0.25, 0.50$ – the latter being the Λ-symmetric point $\tilde{\Delta}_{13}$. In both cases we note (i) D always extrapolates in the thermodynamic limit to a finite value $\mathcal{O}(1)$ and (ii) the fluxed cases, for finite L, always gives larger D values. The second point is analogous to the observation that in the GCE odd-length chains have larger D values than even-length chains.[7] The reason behind such a difference lies mainly in the presence/absence of spin-inversion symmetry (for odd-length chains spin-inversion is always broken). Indeed, as pointed out above, in the absence of spin-inversion all eigenstates, whether degenerate or not, of the XXZ Hamiltonian are connected by the current and give a finite contribution to D. If the states have a definite z-signature, in contrast, many of the eigenstates of H, as e.g. all states with $m_z = 0$ for $\Delta \neq \tilde{\Delta}_{MN}$, carry no current. Hence, D assumes greater values in the GCE for either fluxed or odd-length periodic chains.

Let us focus on $\Delta = 0.5$ first. We see that independent of keeping or breaking the discrete symmetries and the type of ensemble chosen, the D values always agree with one another, even for moderately small $L \approx 18$. Pivotally, they tend to extrapolate to the same value in the thermodynamic limit which is in good agreement with the exactly computed lower bound,[11,12] marked with a cross in the figure. Note that for $\Delta = 0.5$ the lower bound, Eq. (8), and our numerics of Fig. 2, also agree with the Thermodynamic Bethe Ansatz solution[9,20,21]

$$\beta^{-1}D = 2\pi \frac{\gamma - \sin(2\gamma)/2}{16\gamma}, \qquad (9)$$

with $\gamma = \cos^{-1}(0.5) = \pi/3$.

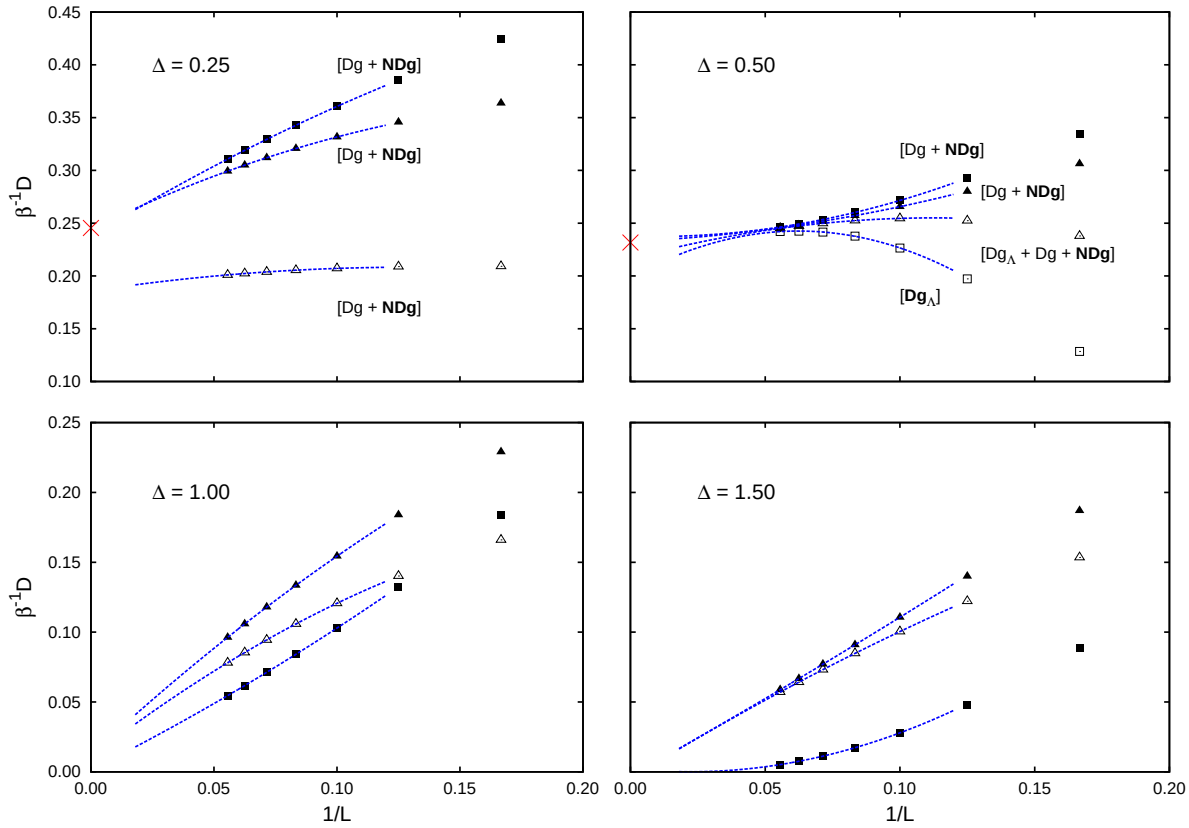

FIG. 2: Finite size scaling of the Drude weight for different values of the anisotropy Δ, calculated within both canonical (CE) and grand canonical ensemble (GCE), and in the presence and absence of a magnetic flux. Symbol coding: ▲ GCE with flux, △ GCE without flux, ■ CE with flux and □ CE without flux. The dashed lines correspond to second order polynomial fits and are to be taken as guide to eye. Top panels show results for the gapless phase, with the crosses representing exact results in the thermodynamic limit,[11,12] and the type of current carrying states that contribute to the finite-L D values labeled as nondegenerate (NDg), degenerate (Dg), and Λ-degenerate states (Dg_Λ); the dominant contributor is highlighted in bold. Bottom panels show results away from gapless phase, consistent with vanishing Drude weight for $L \to \infty$, independent of ensemble or symmetry.

For the second case of $\Delta = 0.25$, which is not *exactly* equal to one of the $\tilde{\Delta}_{MN}$ points (although it can come arbitrarily close to one) the results seem generally the same but distinctly different in one aspect: the finite-size data for the GCE without flux seems to extrapolate to a different thermodynamic limit from the fluxed GCE or CE cases. The latter two here tend to extrapolate to the same thermodynamic limit in good agreement with the exactly lower-bounded result.[11] We understand the source of the discrepancy between non-fluxed GCE and fluxed GCE/CE – as well as to theoretical predictions – as follows: consider the nearby Λ symmetric point $\tilde{\Delta}_{13,31} = \cos(13\pi/31) \approx 0.2506$. For the system sizes considered here the difference $D[\Delta = 0.25] - D[\tilde{\Delta}_{13,31}]$ is always of the order of 10^{-4}. However, we know from the previous section that for $\tilde{\Delta}_{13,31}$ the degeneracies due to the Λ symmetry start showing up for spin chains of length $L \geq 2 \times 31 = 64$. We also know that these degenerate states, the number of which increases with system size, carry a finite current. Thus in order to see the GCE non-fluxed data for $\tilde{\Delta}_{13,31}$ extrapolate to the exact result one would have to consider chains of length $L \geq 64$. Such system sizes are out of the question when all exact eigenstates are needed.

We believe this reasoning may account for the low-ω anomalies observed previously in the convergence of the integrated conductivity at this Δ value,[9] even if in that work spin-inversion was always broken.

Going back to the $\Delta = 0.5$ example, the degeneracies from the Λ symmetry are already present for chains of length $L \geq 6$. This is why we see how, when increasing system size, both non-fluxed GCE and CE data approach the exact lower bound from below. The problem with $\Delta = 0.25$ is that as one chooses $\tilde{\Delta}_{MN}$ points closer to it, the integer N gets significantly large and the corresponding $D[\tilde{\Delta}_{MN}]$ converges towards its exact value very slowly. This of course does not answer the question whether the actual (non-fluxed) GCE data at exactly $\Delta = 0.25$, or any $\Delta \neq \tilde{\Delta}_{MN}$ for that matter, where no Λ symmetry is present, converges towards some

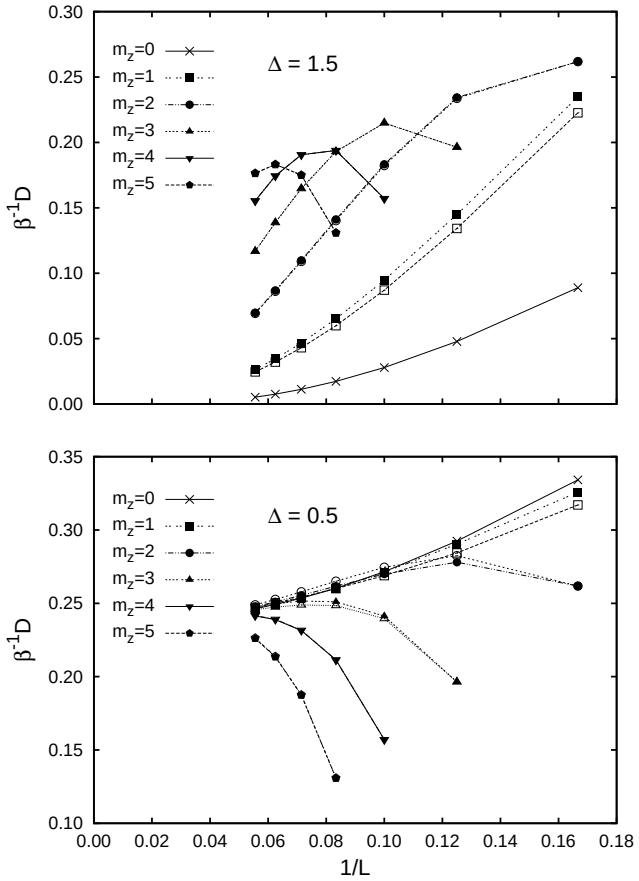

FIG. 3: Finite size scaling of the Drude weight in the canonical ensemble for two Δ values, calculated in the presence (full symbols) and absence (empty symbols) of a magnetic flux, for different magnetization sectors. Crosses indicate $m_z = 0$ values in the presence of a flux. As m_z and L increase the effect of flux disappears for both anisotropies; however note that for larger Δ the $m_z = 0$ contributes the least, whereas it is the opposite for smaller Δ, explaining why, when the weighted average is taken, $m_z = 0$ CE is above (below) the GCE result as seen in the upper (lower) right panel of Fig. 2 for the two anisotropies.

(M, N)-dependent lower bound.

Isotropic point and gapped phase. — Away from the gapless phase the high-temperature Drude weight is expected to vanish.[7,22–24] We confirm this picture holds for GCE and CE, again with and without a flux, in the bottom panels of Fig. 2.

For $\Delta \geq 1$ the quantum symmetry Λ is absent[14,15] and the non-fluxed CE with $m_z = 0$ case gives once more identically zero D due to spin-inversion (and hence it is not shown). Accordingly, and as in the previous subsection, the fluxed GCE results, which include finite contributions from the zero magnetization sector, are above the non-fluxed ones.

The main difference one notes here, in contrast to the two gapless points from above, is that the $m_z = 0$ CE D values are lower than those for the GCE (with and without a flux). This is so because, for these anisotropies and available system sizes, the contributions from the symmetry sectors of finite magnetization densities dominate the summation in Eq. (1), as exemplified by Fig. 3 for $\Delta = 1.5$ (top panel), whereas the trend is exactly the opposite for the smaller anisotropy $\Delta = 0.5$ (bottom panel). Therefore (i) increasing the anisotropy makes the GCE computation less susceptible to the physics of the zero-magnetization sector. From Fig. 3 one also sees (ii) the larger m_z sectors, for which there is no spin-inversion, show less dependence on presence or absence of the flux, simply because the number of pairwise degenerate state of opposite parity is very small, as compared to the size of the corresponding magnetization sector. Points (i) and (ii) account for why the GCE results show less dependence on flux, and hence on $\hat{Z}$ and $\hat{P}$ (and Λ if $\Delta < 1$), when increasing Δ, as was seen in Fig. 2.

IV. SUMMARY

We studied the influence of discrete symmetries (namely parity and spin-inversion) and ensemble (canonical or grand canonical) on the high temperature Drude weight in the anisotropic XXZ chain. Introducing a flux provides a convenient way to break these symmetries and to study their effect upon the numeric evaluation of the Drude weight. We found that when spin-inversion symmetry is broken the dominant contributions to the Drude weight come from the nondegenerate states. In contrast, if spin-inversion is intact only degenerate states related to the Λ quantum symmetry contribute to D; these degeneracies only appear for spin chains of length $L \geq 2N$, for anisotropies $\Delta = \cos(M\pi/N)$ with $N \in \mathbb{Z}^+$ and $M < N$. These observations allowed us to identify the finite-size discrepancies between GCE computations for even- and odd-length chains reported in the literature as consequence of the absence/presence of spin-inversion symmetry in the model.

We found that within the gapless phase $\Delta < 1$ and in the presence of a flux (i.e. when spin-inversion is broken) the finite-size Drude weight extrapolates to the recently computed lower-bounds and exact values, independent of the ensemble used. In contrast, for the non-fluxed case the large-current-carrying degenerate states related to the Λ symmetry only show up for system sizes $L \geq 2N$, where N can be large depending on the anisotropy. This symmetry plays an important role in contributing to the thermodynamic limit of D. Hence, slow convergence towards the exact value should be expected for generically chosen Δ values in the absence of a flux. Therefore if all symmetries are broken, say with a flux, then convergence to the thermodynamic limit is significantly improved.

Away from the gapless phase we confirm absence of ballistic transport for $\Delta \geq 1$, both in the grand canonical ensemble and the zero magnetization sector, with or

without the discrete symmetries preserved.

Finally, we found that with increasing anisotropy the contribution to the Drude peak from the zero magnetization sector goes from being the most dominant to the least dominant. Given that only this magnetization sector is affected by the $\hat{Z}$ symmetry, the role of this decreases with increasing the anisotropy in a grand canonical ensemble calculation.

We thank V. Oganesyan for related collaboration, and B. Doyon, F. Heidrich-Meisner, T. Prosen, V. Rittenberg, and M. Žnidarič for discussions, and the latter for helpful comments on the manuscript.

[1] W. Kohn. *Phys. Rev.*, 133:A171–A181, 1964.
[2] H. Castella, X. Zotos, and P. Prelovsek. *Phys. Rev. Lett.*, 74:972, 1995.
[3] X. Zotos and P. Prelovsek. *Phys. Rev. B*, 53:983, 1996.
[4] X. Zotos, F. Naef, and P. Prelovsek. *Phys. Rev. B*, 55:11029–11032, 1997.
[5] P Mazur. *Physica*, 43:533, 1969.
[6] B. N. Narozhny, A. J. Millis, and N. Andrei. *Phys. Rev. B*, 58:R2921, 1998.
[7] F. Heidrich-Meisner, A. Honecker, D. C. Cabra, and W. Brenig. *Phys. Rev. B*, 68:134436, 2003.
[8] S. Mukerjee and B. S. Shastry. *Phys. Rev. B*, 77:245131, 2008.
[9] J. Herbrych, P. Prelovsek, and X. Zotos. *Phys. Rev. B*, 84:155125, 2011.
[10] V. K. Varma and R. J. Sánchez. *Phys. Rev. A*, 92:013618, 2015.
[11] T. Prosen and E. Ilievski. *Phys. Rev. Lett.*, 111:057203, 2013.
[12] E. Ilievski and J. De Nardis. *arXiv: 1702.02930*, 2017.
[13] A. W. Sandvik. *AIP Conf. Proc*, 1297:135, 2010.
[14] T. Deguchi, K. Fabricius, and McCoy M. *J. Stat. Phys.*, 102:701, 2001.
[15] D. Braak and N. Andrei. *J. Stat. Phys.*, 105(3):677–709, 2001.
[16] K. Kudo and T. Deguchi. *Phys. Rev. B*, 68:052510, 2003.
[17] J. M. P. Carmelo, T. Prosen, and D. K. Campbell. *Phys. Rev. B*, 92:165133, 2015.
[18] M. Rigol and B. S. Shastry. *Phys. Rev. B*, 77:161101, 2008.
[19] T. Prosen. *Phys. Rev. Lett.*, 106:217206, 2011.
[20] X. Zotos. *Phys. Rev. Lett.*, 82:1764, 1999.
[21] J. Benz, T. Fukui, A. Kluemper, and C. Scheeren. *J. Phys. Soc. Jpn. Supp.*, 74:181, 2005.
[22] M. Znidaric. *Phys. Rev. Lett.*, 106:220601, 2011.
[23] M. Znidaric. *Phys. Rev. B*, 90:115156, 2014.
[24] M. Znidaric, A. Scardicchio, and V. K. Varma. *Phys. Rev. Lett.*, 117:040601, 2016.